

Synthesis of Mesoporous Aromatic Silica Thin Films and Their Optical Properties

Yasutomo Goto,^{†,‡} Norihiro Mizoshita,^{†,‡} Osamu Ohtani,[†] Tadashi Okada,^{‡,§}
Toyoshi Shimada,^{‡,||} Takao Tani,^{†,‡} and Shinji Inagaki^{*,†,‡}

Toyota Central R&D Laboratories, Inc., Nagakute, Aichi 480-1192, Japan, Core Research and Evolutional Science and Technology (CREST), Japan Science and Technology (JST), Kawaguchi, Saitama 332-0012, Japan, Toyota Physical & Chemical Research Institute, Nagakute, Aichi 480-1192, Japan, and Department of Chemical Engineering, Nara National College of Technology, Yamatokoriyama, Nara 639-1080, Japan

Received December 11, 2007. Revised Manuscript Received April 8, 2008

Various aromatic-bridged periodic mesoporous organosilica (PMO) thin films were prepared from 100% organosilane precursors containing bridging organics of 1,4-phenylene (Ph), 4,4'-biphenylene (Bp), 2,6-naphthylene (Nph), and 9,10-anthrylene (Ant) by an evaporation-induced self-assembly approach. Structural and optical properties of the films were characterized. Transparent films with periodic mesostructures were successfully obtained for all the compositions. The absorption spectra of the PMO films were similar to those of their precursors, indicating little interaction between the aromatic groups in the frameworks in the ground state, whereas the fluorescence spectra of the PMO films significantly red-shifted and also broadened compared with those of their precursors, suggesting excimer formation in the excited state. The quantum yields of the Ph-, Nph-, and Ant-PMO films were lower than those of their precursors by solid-state quenching. Exceptionally, the quantum yield increased above that of the precursor for the Bp-PMO film in spite of excimer formation. The high absorption coefficient ($87\,000\text{ cm}^{-1}$) and high quantum yield (0.45) of the Bp-PMO film indicate its great potential for use as fluorescent materials.

Introduction

Periodic mesoporous organosilicas (PMOs), synthesized from 100% or less organic-bridged organosilane precursors $[(R'O)_3Si-R-Si(OR')_3]$, are a new class of materials having well-defined nanoporous structure and framework functionalities attributed to organic groups in their pore walls.¹ PMOs have attracted much attention owing to their potential use in various applications such as catalysts,² adsorbents,³ and optical devices.⁴ PMOs are particularly suitable for optical applications in which a large amount of organic chromophores can be incorporated within their pore walls. PMOs containing a large amount of chromophores are expected to show a high absorption efficiency of light and unique optical properties due to the densely packed chromophores in their framework. Although several PMOs containing framework organic chromophores, such as viologen,⁵ bispyridylethyl-

ene,⁶ triphenylpyrylium,⁷ Ru and Eu complexes,⁴ and azobenzene⁸ moieties, have been reported so far, these were prepared by co-condensation with a large amount of a pure silica precursor, such as tetraethoxysilane (82–99 mol %). The co-condensation approach resulted in dilution of the organic chromophores in the framework with silica. PMOs prepared from 100% bridged organosilane precursors have been reported for organic chromophores, such as phenylene,⁹ biphenylene,¹⁰ thiophene,¹¹ diacetylene,¹² and carbazole.¹³ However, optical properties of these PMOs have not been studied in detail.

Especially for optical applications, transparent film-shaped PMOs^{14,15} are advantageous compared with powder-shaped PMOs because of easy shaping (patterning) and low optical loss (no light scattering). Here, we focus on transparent film-shaped PMOs and synthesized PMO films from 100% organosilane precursors containing bridging organics of 1,4-phenylene (Ph), 4,4'-biphenylene (Bp), 2,6-naphthylene (Nph), and 9,10-anthrylene (Ant). Although the synthesis of

* To whom correspondence should be addressed. E-mail: inagaki@mosk.tytlabs.co.jp.

[†] Toyota Central R&D Laboratories, Inc.

[‡] Japan Science and Technology (JST).

[§] Toyota Physical & Chemical Research Institute.

^{||} Nara National College of Technology.

- (1) (a) Inagaki, S.; Guan, S.; Fukushima, Y.; Ohsuna, T.; Terasaki, O. *J. Am. Chem. Soc.* **1999**, *121*, 19611. (b) Melde, B. J.; Holland, B. T.; Blanford, C. F.; Stein, A. *Chem. Mater.* **1999**, *11*, 3302. (c) Asefa, T.; MacLachlan, M. J.; Coombs, N.; Ozin, G. A. *Nature* **1999**, *402*, 867.
- (2) Yang, Q.; Liu, J.; Yang, J.; Kapoor, M. P.; Inagaki, S.; Li, C. *J. Catal.* **2004**, *228*, 265.
- (3) Rebbin, V.; Schmidt, R.; Fröba, M. *Angew. Chem., Int. Ed.* **2006**, *45*, 5210.
- (4) Minoofar, P. N.; Hernandez, R.; Chia, S.; Dunn, B.; Zink, J. I.; Franville, A.-C. *J. Am. Chem. Soc.* **2002**, *124*, 14388.
- (5) Alvaro, M.; Ferrer, B.; Fornes, V.; Garcia, H. *Chem. Commun.* **2001**, 2546.

- (6) Alvaro, M.; Ferrer, B.; Garcia, H.; Rey, F. *Chem. Commun.* **2001**, 2012.
- (7) Alvaro, M.; Aprile, C.; Benitez, M.; Bourdelande, J. L.; Garcia, H.; Herance, J. R. *Chem. Phys. Lett.* **2005**, *414*, 66.
- (8) Besson, E.; Mehdi, A.; Lerner, D. A.; Reye, C.; Corriu, R. J. P. *J. Mater. Chem.* **2005**, *15*, 803.
- (9) Inagaki, S.; Guan, S.; Ohsuna, T.; Terasaki, O. *Nature* **2002**, *416*, 304.
- (10) Kapoor, M. P.; Yang, Q.; Inagaki, S. *J. Am. Chem. Soc.* **2002**, *124*, 15176.
- (11) Morell, J.; Wolter, G.; Fröba, M. *Chem. Mater.* **2005**, *17*, 804.
- (12) Peng, H.; Tang, J.; Yang, L.; Pang, J.; Ashbaugh, H. S.; Brinker, C. J.; Yang, Z.; Lu, Y. *J. Am. Chem. Soc.* **2006**, *128*, 5304.
- (13) Maegawa, Y.; Goto, Y.; Inagaki, S.; Shimada, T. *Tetrahedron Lett.* **2006**, *47*, 6957.

Ph-PMO (nanoparticle,¹⁴ film,¹⁵ powder⁹) and Bp-PMO (powder¹⁰) has already been reported, the synthesis of Nph- and Ant-PMOs is first reported in this study. Structural and optical properties of the films were characterized. Transparent films with periodic mesostructures were obtained for all of the compositions. The PMO films showed high absorption efficiency and excimer emissions at significantly red-shifted wavelengths owing to the densely packed chromophores in their frameworks. Exceptionally, the Bp-PMO film showed a high fluorescence quantum yield ($\Phi = 0.45$), which was higher than that ($\Phi = 0.35$) of its precursor solution.

Experimental Section

General Details. All reagents and solvents were of the highest commercial quality and used without further purification. A cationic surfactant, C₁₈TMACl (C₁₈H₃₇N⁺(CH₃)₃Cl⁻), and a nonionic surfactant, Brij-76 (C₁₈H₃₇(OCH₂CH₂)₁₀OH), were purchased from TCI and Aldrich, respectively. 1,4-Bis(triethoxysilyl)benzene and 4,4'-bis(triethoxysilyl)biphenyl were obtained from Nard Institute, Ltd. 9,10-Bis(triethoxysilyl)anthracene¹⁶ was bought from AZmax Co., Ltd. 2,6-Bis(triethoxysilyl)naphthalene was synthesized by Rh-catalyzed silylation as shown below. ¹H and ¹³C NMR spectra were measured by using JEOL JNM-LA500 spectrometer. High resolution mass spectroscopy (HRMS) was performed on a JEOL JMS-700 spectrometer.

Synthesis of Nph-Based Precursor. A mixture of 2,6-dibromonaphthalene (1.00 g, 3.50 mmol), [Rh(CH₃CN)₂(cod)]BF₄ (66.4 mg, 0.18 mmol), tetrabutylammonium iodide (2.59 g, 7.00 mmol), dimethylformamide (25 mL), and triethylamine (2.94 mL) was cooled to 0 °C. After adding triethoxysilane (2.60 mL, 14.06 mmol), the mixture was stirred at 80 °C for 2 h. The reaction mixture was concentrated under reduced pressure and then extracted with ether. The organic phase was filtrated using Celite, and the solvent was removed by rotary evaporator and in vacuum. Purification of the residue by reduced-pressure distillation gave 2,6-bis(triethoxysilyl)naphthalene as a transparent oil (0.73 g, 46%). ¹H NMR δ (ppm, CDCl₃, 500 MHz) = 8.22 (s, 2H), 7.89 (d, $J = 8.1$ Hz, 2H), 7.74 (d, $J = 8.1$ Hz, 2H), 3.92 (q, $J = 7.0$ Hz, 12H), 1.28 (t, $J = 7.0$ Hz, 18H). ¹³C NMR δ (ppm, CDCl₃, 125.7 MHz) = 136.0, 133.6, 130.4, 129.6, 127.5, 58.8, 18.2. HRMS (FAB⁺, m/z) calcd for C₂₂H₃₆O₆Si₂, 452.2050 [M]⁺; found, 452.2049.

Preparation of the PMO Films. The PMO films were prepared by an evaporation-induced self-assembly approach. The organosilane precursors were mixed with the surfactants, hydrochloric acid (2 N), deionized water, and solvents at optimized ratios (Table 1), forming transparent sol solutions. The compositions of the sol solutions are summarized in Table 1. After stirring at room temperature for 2–12 h the sol-solutions were coated on quartz glass plates by spin-coating at 4000 rpm for 30 s, followed by drying in vacuum at room temperature, yielding Ph-, Bp-, Nph-, and Ant-PMO films (Figure 1). Transparent and uniform films were obtained for all the compositions. Thicknesses were 710, 550, 340, and 130 nm for Ph-, Bp-, Nph-, and Ant-PMO films, respectively. The thickness varied with precursor concentration (solubility) and viscosity of the sol solutions. In this study, the surfactant was not extracted from the PMO films to suppress fluorescence quenching by oxygen.

Table 1. Compositions of the Sol Solutions Used for Preparing the Ph-, Bp-, Nph-, and Ant-PMO Films

| | precursor | surfactant | HCl (2 N) | water | solvent |
|----------------------|-----------|--------------------------------|-------------|-------------|---------------------------|
| Ph-PMO ^a | 1 g | C ₁₈ TMACl (0.35 g) | 10 μ L | 360 μ L | ethanol 1 g |
| Bp-PMO ^a | 0.6 g | Brij-76 (0.43 g) | 10 μ L | 180 μ L | ethanol 2 g |
| Nph-PMO ^a | 0.9 g | C ₁₈ TMACl (0.6 g) | 40 μ L | 400 μ L | ethanol 6 g |
| Ant-PMO ^b | 0.05 g | Brij-76 (0.043 g) | 2.5 μ L | 22 μ L | THF (1 g) + ethanol (1 g) |

^a The solutions were diluted with water (1 g) + ethanol (1 g), water (0.1 g) + ethanol (3 g), and ethanol (4 g) just before spin coating to optimize their viscosity for the Ph-, Bp-, and Nph-PMO film preparation, respectively. ^b Amounts of HCl and water were much decreased to suppress cleavage of the Si–C bondings for preparation of the sol solution for Ant-PMO.

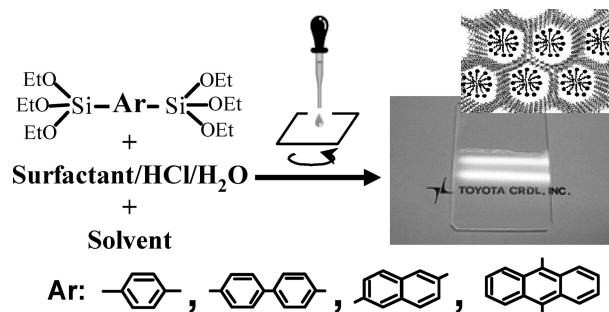


Figure 1. Preparation of aromatic-bridged PMO films from various bridged organosilane precursors by an evaporation-induced self-assembly approach.

Characterization of the PMO Films. The periodicity of the mesostructure was determined by XRD (Rigaku RINT-TTR) using Cu K α radiation (50 kV, 300 mA) and transmission electron microscopy (TEM; JEOL EX2000, 200 kV). The bonding state was characterized by ²⁹Si magic angle spinning nuclear magnetic resonance (MAS NMR). The UV–vis absorption spectrum was obtained with a spectrophotometer (JASCO V-670). The fluorescence spectrum was measured by a spectrofluorometer (JASCO FP6500). The fluorescence quantum yield was evaluated using an Absolute Photoluminescence Quantum Yield Measurement System (Hamamatsu Photonics C9920-02). Prior to measurements, quantum yields of naphthalene in cyclohexane and anthracene in ethanol were evaluated and confirmed to be identical to the literature values (0.23 and 0.27 for naphthalene and anthracene, respectively).¹⁷ All measurements for solution samples were carried out after argon gas bubbling for at least 10 min to remove oxygen in the solutions for suppression of quenching by oxygen.

Results and Discussion

Structural Properties. Figure 2 shows X-ray diffraction (XRD) patterns of the PMO films. Intense peaks were observed at 2.16, 1.46, 2.44, and 1.36°, corresponding to d -spacings of 4.1, 6.1, 3.6, and 6.5 nm, for the Ph-, Bp-, Nph-, and Ant-PMO films, respectively, indicating periodic mesostructures in the films. No sharp peaks were observed at 5–60° for all the PMO films, suggesting no crystal-like ordered structures of the organic groups within the pore walls, unlike the Ph- and Bp-PMO powders.^{9,10} Figure 3 shows a TEM image of the Ph-PMO film. Mesostructures with a periodicity of about 4 nm were observed clearly. The periodicity was in good agreement with that expected on the basis of the XRD results (4.1 nm: Figure 2). For the other films, TEM observation was difficult because of collapse of

(14) Lu, Y. F.; Fan, H. Y.; Doke, N.; Loy, D. A.; Assink, R. A.; LaVan, D. A.; Brinker, C. J. *J. Am. Chem. Soc.* **2000**, *122*, 5258.

(15) Dag, O.; Yoshina-Ishii, C.; Asefa, T.; MacLachlan, M. J.; Grondy, H.; Coombs, N.; Ozin, G. A. *Adv. Funct. Mater.* **2001**, *11*, 213.

(16) (a) Shea, K. J.; Loy, D. A.; Webster, O. *J. Am. Chem. Soc.* **1992**, *114*, 6700. (b) Loy, D. A.; Shea, K. J. *Chem. Rev.* **1995**, *95*, 1431.

(17) Berlman I. B. *Handbook of Fluorescence Spectra of Aromatic Molecules*; Academic Press: New York, 1971.

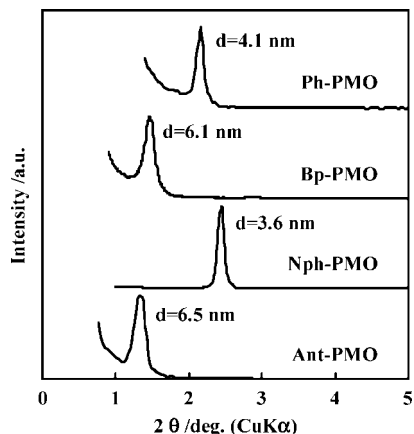


Figure 2. XRD patterns of benzene (Ph)-, biphenyl (Bp)-, naphthalene (Nph)-, and anthracene (Ant)-PMO films.

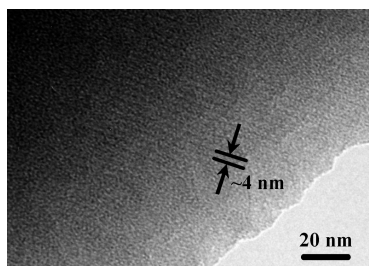


Figure 3. TEM image of the benzene-PMO film calcined at 250 °C.

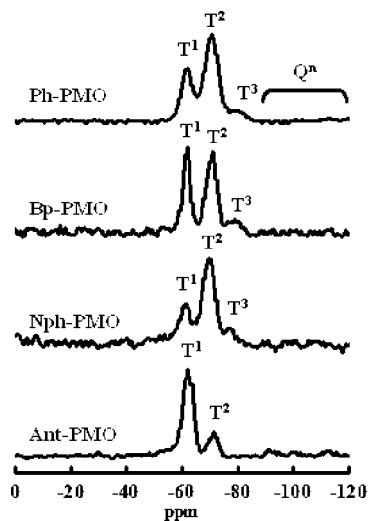


Figure 4. ^{29}Si MAS NMR spectra of benzene (Ph)-, biphenyl (Bp)-, naphthalene (Nph)-, and anthracene (Ant)-PMO films.

the mesostructures by irradiation of electron beam. Figure 4 shows ^{29}Si MAS NMR spectra of the PMO films. The peaks in each spectrum were assigned to T^n [$\text{R-Si}(\text{OH})_{3-n}(\text{OSi})_n$, $n = 0-3$] species, and almost no peaks were observed from -90 to -120 ppm, indicating absence of Q^n [$\text{Si}(\text{OH})_{4-n}(\text{OSi})_n$, $n = 0-4$] species. These results suggest that siloxane networks were formed without cleavage of Si–C bonds during the synthesis process for all the PMO films. The degrees of condensation were lower for the PMO films than those for the PMO powders^{9,10} synthesized at 95 °C because of the mild synthesis conditions.

Optical Properties. Figure 5 shows absorption spectra of the PMO films and their precursors in 2-propanol ($\sim 10^{-5}$

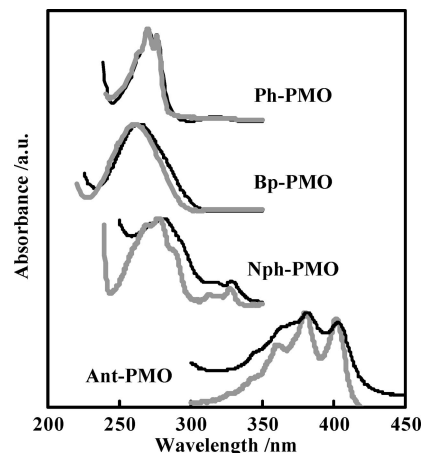


Figure 5. Absorption spectra of benzene (Ph)-, biphenyl (Bp)-, naphthalene (Nph)-, and anthracene (Ant)-PMO films and their precursors in 2-propanol ($\sim 10^{-5}$ M).

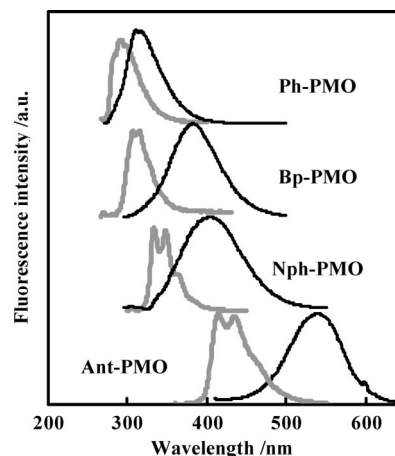


Figure 6. Fluorescence spectra of benzene (Ph)-, biphenyl (Bp)-, naphthalene (Nph)-, and anthracene (Ant)-PMO films and their precursors in 2-propanol ($\sim 10^{-5}$ M).

M). The absorption bands for all the PMO films had almost the same shape as those of their precursor solutions. The results indicate little interaction between the aromatic groups in the frameworks in the ground state despite of their dense packing structure. On the other hand, a red shift of absorption spectra is observed in aromatic-PMO powders.¹⁸ As seen in the NMR spectra (Figure 4), sol-gel synthesis at room temperature resulted in insufficient condensation and thus relatively loosely packed structures in the PMO films compared with the PMO powders, which may rather isolate the aromatic groups in the PMO films.

Figure 6 shows fluorescence spectra of the PMO films and the diluted solutions of their precursors. The fluorescence bands of the PMO films shifted significantly to longer wavelengths and also broadened from the fluorescence bands of precursor solutions, suggesting strong interaction (excimer formation) between the aromatic groups in the excited state. A similar behavior has been observed by Shea et al. who compared fluorescence emission and excitation spectra of the nonporous 9,10-anthracene–silica hybrid gel with those of its precursor (9,10-bis(triethoxysilyl)anthracene) and found significant red-

(18) Unpublished results.

Table 2. Absorption Coefficients (α) and Fluorescence Quantum Yields (Φ) of the Films and Molar Extinction Coefficients (ϵ) and Φ of the Precursors in 2-Propanol

| | α , 10^4 cm^{-1} (at λ , nm) | ϵ , $10^4 \text{ M}^{-1} \text{ cm}^{-1}$ (at λ , nm) | Φ (excited at λ , nm) | |
|---------|--|---|------------------------------------|------------|
| | film | precursor | film | precursor |
| Ph-PMO | 0.57 (270) | 0.092 (270) | 0.03 (266) | 0.07 (266) |
| Bp-PMO | 8.7 (263) | 5.7 (260) | 0.45 (266) | 0.35 (270) |
| Nph-PMO | 2.4 (282) | 0.38 (278) | 0.09 (266) | 0.33 (280) |
| Ant-PMO | 1.4 (382) | 2.6 (380) | 0.07 (380) | 0.92 (360) |

shift only in the emission spectrum.^{16a} A monomeric emission in addition to the broad emission was observed in fluorescence spectrum of the Bp-PMO film (Figure S1, Supporting Information) at 77 K, suggesting that the excimer formation is partially suppressed at low temperatures. On the other hand, such behaviors are not observed in organic crystals (biphenyl,¹⁹ naphthalene,²⁰ and anthracene²¹) where monomeric fluorescence is observed, implying that configuration of the aromatic groups in the aromatic-PMO films differs from those in the aromatic single crystals. The energies of the fluorescence shift between the PMO films and the precursors were approximately 0.41, 0.81, 0.63, and 0.72 eV for Ph-, Bp-, Nph-, and Ant-PMOs, respectively. Table 2 tabulates absorption coefficients (α) and fluorescence quantum yields (Φ) of the PMO films as well as molar extinction coefficients (ϵ) and fluorescence quantum yields of the precursors. The absorption coefficients of the PMO films varied from 5700 to 87 000 cm^{-1} , and the Bp-PMO film showed the highest value among the PMO films in this study because its precursor had the highest molar extinction coefficient. The quantum yields of the Ph-, Nph-, and Ant-PMO films were lower than those of their precursors (Ph, 0.07 \rightarrow 0.03; Nph, 0.33 \rightarrow 0.09; Ant, 0.92 \rightarrow 0.07), which can be explained by the strong interaction in the excited state between the aromatic groups (so-called solid-state quenching) as seen in the fluorescence spectra (Figure 6). It is worth noting that the quantum yield increased exceptionally above that of the precursor for the Bp-PMO film ($\Phi = 0.35 \rightarrow 0.45$) in spite of the excimer formation. Similarly, a quantum yield of the Bp-PMO powder increases from that of its precursor.¹⁸ Enhancement of fluorescence by aggregation is well-known as aggregation-induced enhanced emission and has been observed in organic molecules,²² polymers,²³ and nanoparticles²⁴ but has not been reported in covalently bridged organic-inorganic hybrid materials including PMOs. It has been proposed that

intramolecular planarization and/or restriction of intramolecular rotation can promote aggregation-induced emission. Among the aromatic groups in this study, only a biphenyl group shows large conformational change by excitation where two phenyl rings twist for 44° in the ground state and is planarized in the excited state.²⁶ However, the present result cannot be explained by intramolecular planarization in the ground state because planarization of phenyl rings results in a red-shift of the absorption band,²⁵ which was not seen in this study (Figure 5). The intramolecular rotational vibration of the biphenyl group might be restricted by the dense packing structure for the Bp-PMO film, which would be one of the reasons for unusual improvement of the quantum yield. On the other hand, excimer formation of biphenyl species has not been usually observed for the molecule system due to the steric hindrance of the twisted phenyl ring structure. Recently, excimer formation has been reported for some special cases such as biphenyl molecule adsorbed on clays,²⁷ biphenyl-bridged cyclodextrin dimer,²⁸ and biphenyl-pillared layered hybrid material.²⁹ But, no results on quantum efficiency of the biphenyl species have been reported in their studies.

Summary

In this study, various aromatic-PMO films were prepared from 100% organosilane precursors containing bridging organics of Ph, Bp, Nph, and Ant groups by an evaporation-induced self-assembly approach. Transparent films with periodic mesostructures were successfully obtained for all the compositions. The NMR results confirmed a formation of siloxane networks without cleavage of the Si-C bond during the synthesis process. The absorption spectra of the PMO films were similar to those of diluted solution of their precursors, indicating little interaction between the aromatic groups in the frameworks in the ground state. On the other hand, the fluorescence spectra of the PMO films significantly red-shifted and also broadened compared with those of their precursor solutions, suggesting excimer formation. The quantum yields of the Ph-, Nph-, and Ant-PMO films were lower than those of their precursors by solid-state quenching. Exceptionally, the quantum yield increased above that of the precursor for the Bp-PMO film in spite of excimer formation. This is the first example of aggregation-induced enhanced emission for covalently bridged organic-inorganic hybrid materials including PMOs. The high absorption coefficient (87 000 cm^{-1}) and high quantum yield (0.45) of the Bp-PMO film indicate its great potential for use as fluorescent materials.

Supporting Information Available: Fluorescence spectra of the Bp-PMO film at room temperature and 77 K (PDF). This material is available free of charge via the Internet at <http://pubs.acs.org>.

CM800492S

- (19) Huang, H. W.; Horie, K.; Yamashita, T.; Machida, S.; Sone, M.; Tokita, M.; Watanabe, J.; Maeda, Y. *Macromolecules* **1996**, *29*, 3485–3490.
- (20) Selvakumar, S.; Sivaji, K.; Arulchakkaravarthi, A.; Balamurugan, N.; Sankar, S.; Ramasamy, P. *J. Cryst. Growth* **2005**, *282*, 370.
- (21) Dreger, Z. A.; Lucas, H.; Gupta, Y. M. *J. Phys. Chem. B* **2003**, *107*, 9268.
- (22) (a) Luo, J. D.; Xie, Z. L.; Lam, J. W. Y.; Cheng, L.; Chen, H. Y.; Qiu, C. F.; Kwok, H. S.; Zhan, X. W.; Liu, Y. Q.; Zhu, D. B.; Tang, B. Z. *Chem. Commun.* **2001**, 1740. (b) Zeng, Q.; Li, Z.; Dong, Y. Q.; Di, C. A.; Qin, A. J.; Hong, Y. N.; Ji, L.; Zhu, Z. C.; Jim, C. K. W.; Yu, G.; Li, Q. Q.; Li, Z. A.; Liu, Y. Q.; Qin, J. G.; Tang, B. Z. *Chem. Commun.* **2007**, 70.
- (23) Deans, R.; Kim, J.; Machacek, M. R.; Swager, T. M. *J. Am. Chem. Soc.* **2000**, *122*, 8565.
- (24) An, B. K.; Kwon, S. K.; Jung, S. D.; Park, S. Y. *J. Am. Chem. Soc.* **2002**, *124*, 14410.

- (26) Im, H. S.; Bernstein, E. R. *J. Chem. Phys.* **1988**, *88*, 7337.
- (25) Ambroschdraxl, C.; Majewski, J. A.; Vogl, P.; Leising, G. *Phys. Rev. B* **1995**, *51*, 9668.
- (27) Cione, A. P. P.; Scaiano, J. C.; Neumann, M. G.; Gessner, F. J. *Photochem. Photobiol., A* **1998**, *118*, 205–209.
- (28) Sasaki, K.; Nagasaka, M.; Kuroda, Y. *Chem. Commun.* **2001**, 2630–2631.
- (29) (a) Ishii, R.; Shinohara, Y. *J. Mater. Chem.* **2005**, *15*, 551–553. (b) Ishii, R.; Ikeda, T.; Itoh, T.; Ebina, T.; Yokoyama, T.; Hanaoka, T.; Mizukami, F. *J. Mater. Chem.* **2006**, *16*, 4035–4043.